

# Metamorphosis from LCEP to UCEP in the Metastable Three-Phase Region

Paul H. E. Meijer<sup>†</sup>

Physics Department, Catholic University of America, Washington, D.C. 20064

Received: January 21, 1999; In Final Form: March 25, 1999

The behavior of the phase lines in binary gas–liquid systems was classified by van Konynenburg and Scott according to the various connectivities of the critical lines and the three-phase lines, occurring in the pressure–temperature diagrams of such systems. The three-phase line in type IV starts at a (LL)V point and ends at a L(LV) point. Somewhere near this line a transition takes place which determines the outcome at the end of the line. At this changeover point, called the plait-point transformation, two binodal cusps meet each other on the spinodal and at the same time, on the other end of the tieline, two binodals will cross each other and osculate. This phenomenon is described and analyzed in detail and a mathematical description of this behavior is given.

## 1. Introduction: Topology of Binodals

Certain phase diagrams for binary gas–liquid mixtures contain three-phase lines of finite length. Specifically in type V (and also in type IV),<sup>1</sup> one encounters three-phase lines that start at a LCEP (lower critical end point) and end at an UCEP (upper critical end point). In phase diagrams of type VI which also contain a finite segment of a three-phase line, both critical end points are (LL). That is, (LL) returns to (LL), and there is no such exchange.

The general description of this phenomenon is as follows: of the three phases 1, 2, and 3, phases 1 and 2 merge at one end of the three-phase line, while at the other end of the line two different phases, say 2 and 3, merge. This is shown in the  $x(T)$  diagram, the concentration as function of the temperature; see Figure 1, lower part,<sup>2</sup> representing type V.

The sigmoid curve RNOM in the lower part of Figure 1 displays the three densities of the three-phase curve CD in the upper part. The segment RN is the high concentration liquid branch, the segment NO the medium concentration liquid part, and the segment OM the vapor part. At the LCEP at temperature  $T_L$ , which is the point N in the lower figure and the point C in the upper part, the two liquid phases merge. Such a merger can be anticipated by observing the binodals in the complete, that is, including the metastable and unstable parts,  $V(x)$  or  $p(x)$ , plots. The separate loop binodal containing the critical points  $P_1$  (corresponding to the branch TQ in the lower part of Figure 1) and  $P_2$  (corresponding to the branch TV in Figure 2) will first retract into the main bulge (at the LCEP) and then shrink at still lower temperatures by merging these two critical points at the points T and S, the end of the unstable critical line. The conclusion is that the separate binodal loop ( $D''P_2C''P_1$ ) determines the behavior at the end of the three-phase line.

A similar situation occurs below the UCEP (the point O in the lower figure), except that the closed loop binodal is a different one. In Figure 3 it can be seen that the critical point  $P_1$  is now part of the main loop, while the critical points  $P_2$  and  $P_3$  are situated on the secondary loop. The last is positioned on the left, while the previously mentioned secondary loop is positioned on the upper part of the figure. This will lead to a

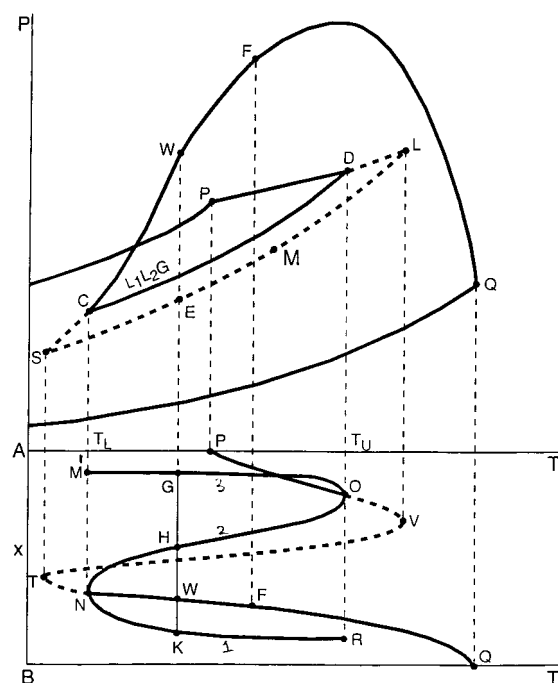


**Figure 1.**  $p(T)$  and  $x(T)$  critical lines of a system of type IV. CD is the three phase line. C is the LCEP with  $(L_1L_2)V$  and D the UCEP with  $L_1(L_2V)$ .

different behavior when the temperature approaches  $T_U$ , the point at which the loop retracted inside the main part of the binodal. Somewhere between  $T_L$  and  $T_U$  the topology of the binodals undergoes a change from the pattern shown in Figure 2 to the pattern shown in Figure 3. Scheffer called this the plait-point transformation. A general description of this phenomenon is given in a paper by Meijer.<sup>3</sup> In this paper (see Figure 1), the plait point is indicated to lie on the unstable part of the critical line, following Scheffer. This is incorrect, as will be discussed below.

The pressure–temperature or  $p(T)$  plot in Figure 1 shows a three-phase line situated between the boiling points of the two components and going from C to D. The lower temperature  $T_L$  of the LCEP is associated with the merging of the two liquid

<sup>†</sup> E-mail: meijer@CUA.edu.

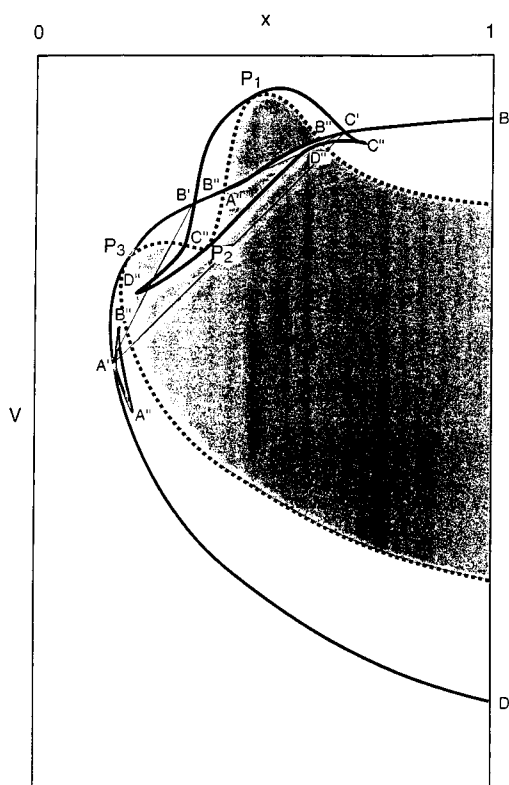


**Figure 2.** Binodals and spinodals before the exchange at  $T_{\text{LCEP}} < T < T_{\text{M}}$ . The main binodal  $BP_3D$  starts and ends at  $x = 1$ ; the binodal  $CP_1D$  forms a closed loop.

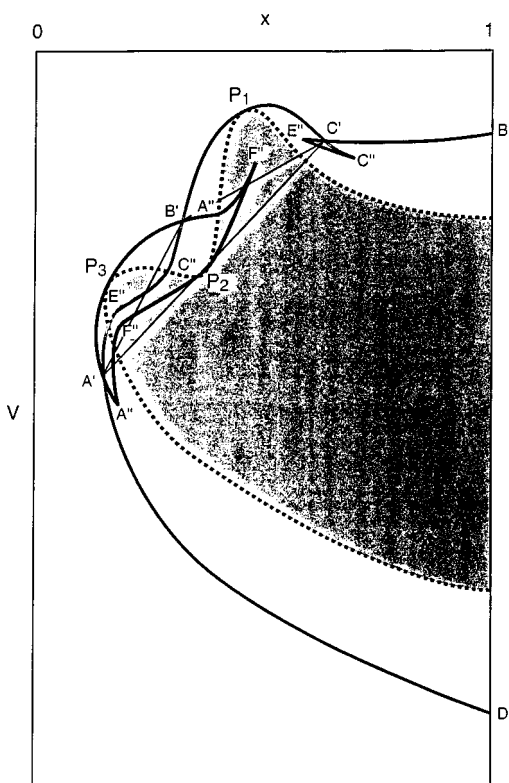


**Figure 3.** Binodals and spinodals after the exchange at  $T_{\text{M}} < T < T_{\text{UCEP}}$ . The main binodal  $BP_1D$  starts and ends at  $x = 1$ ; the binodal  $FP_3A$  forms a closed loop.

phases, while the upper end point D at the temperature  $T_U$  represents the merging of the vapor phase with the liquid of the more volatile component. However, which pair of the three

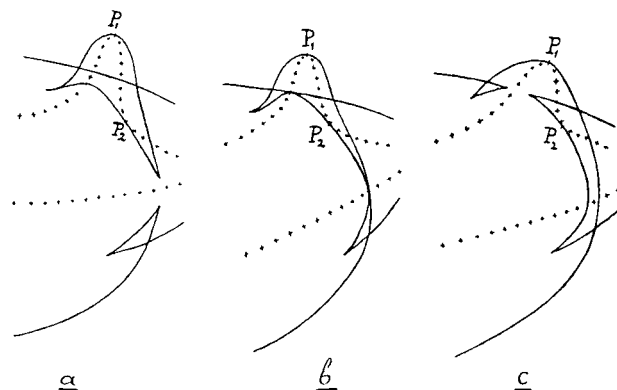


**Figure 4.** Sequence of figures showing the simultaneous exchange mechanism of the binodals (the + signs refer to the spinodal). Reprinted with permission from ref 6. Copyright 1912–1913 Koninklijke Nederlandse Akademie van Wetenschappen.

phases will merge at the end of a three-phase line cannot be observed from the behavior of the line itself, but the changeover can be seen by investigating the metastable parts of the isothermal  $V(x)$  or  $p(x)$  binodal curves. The connectivities of these curves will determine the outcome at the ends of the three-phase line. Such a sequence can be seen in the work of van der Waals<sup>4,5</sup> in a set of  $V(x)$  diagrams before and after the changeover (compare figures 103, 104, 105 also shown in ref 3 as well as figures 125–128). Similar diagrams can be found in the work of Scheffer<sup>6</sup> reproduced as Figure 4. It is not known whether such drawings represent actual numerical calculations or whether they are just sketches, since most of the archival materials are lost. Most likely one deals with the last case.

To describe the situation in more detail, consider Figure 2 taken from ref 2, the  $V(x)$  plot at a temperature  $T$  somewhat above  $T_P$  (the critical temperature of the first component), and far below  $T_Q$  (the critical temperature of the second, less volatile, component). The binodal lines in this figure consist of two (overlapping) disjoint pieces of continuous curves. One curve starts and ends on the  $x = 1$  axis. On the left side, close to the  $x = 0$  axis lies a critical point  $P_3$ . Somewhat below this point the curve contains two cusps, giving rise to a swallowtail-like structure. The other curve, going through  $P_1$ , forms a closed loop and contains two cusps.

The first curve forms the main part of the binodal. It starts at B, on the  $x = 1$  axis, crosses the spinodal at  $B''$  and again at  $A''$ , passes through the critical point  $P_3$ , regresses and advances at the point  $A'$ , and finally returns to the  $x = 1$  axis at point  $D'$ . Each point of the binodal is associated with another point on the binodal by means of a tieline. To show their association, they carry the same label. The tielines and isobars are omitted from the figure in order to avoid too much clutter. The butterfly-like detour at  $A'$  results from the fact that the segment corresponding to  $A''$ – $B''$  lies inside the spinodal where the A-surface has negative curvature. To recapitulate: the binodal consists of two parts, a “bulge” from B to  $D'$ , with a critical point  $P_3$ , and a closed loop with two critical points,  $P_1$  which is stable and  $P_2$ , a critical point in the unstable region. The region inside the spinodal is unstable and the regions between the spinodals and the binodals are metastable.

The relation between the crossings of the binodal with the spinodal at one end and the cusps at the other end of the corresponding tielines is given by the theorems of Korteweg,<sup>7</sup> recently elaborated by Meijer.<sup>8</sup> The closed loop goes, moving counter clockwise, from the cusp  $C''$  via the critical point  $P_1$  to the cusp  $D''$  and back to  $C''$  via the critical point  $P_2$ . Again

each spinodal–binodal crossing is associated with a corresponding cusp. The points  $A'$ ,  $B'$ , and  $C'$  form the three-phase triangle.

If the temperature is raised, a change in the topology of the curves will take place. The transformation can be seen by following the behavior of the two cusps  $D''$  and  $B''$  that are facing each other on each side of the spinodal (see Figure 2, below  $P_3$ ). Upon further changes in the Helmholtz surface (by raising the temperature), these two cusps will meet and form two continuous binodal curves that will cross and osculate, i.e., have the same tangents, at the crossing point with the spinodal. Beyond this point the two binodals will separate, each crossing the spinodal at different points  $E''$  and  $F''$ , see Figure 3 also below  $P_3$ . Simultaneously, at the other end of the tielines, below and to the right of point  $P_1$ , the opposite scenario takes place. When the two crossing points  $B''$  and  $D''$  of the binodal with the spinodal approach each other (see Figure 2), binodals will detach and form two cusps  $F''$  and  $E''$  right and left of the spinodal; see Figure 3. That is, when the cusps on one end meet each other, the crossings at the other end merge. After the cusps have disappeared and become two separated crossings at one end, the other end displays now two opposing cusps with a spinodal in between; hence, one of the two must lie in the unstable region.

After this interchange the connectivity of the network of binodals is different. In Figure 3 the main part goes through  $P_1$  and the critical point  $P_3$  is part of the closed loop with cusps at  $A''$  and  $F''$ . This is still a three-phase state, but if the closed loop retracts inside the main loop, one deals with a different merger of two of the phases. Before the changeover one dealt with a  $V(x)$  diagram that is related to a  $V(L_1L_2)$  type end point of the three-phase line, and after the changeover the three-phase line will eventually end with a  $(VL_1)L_2$  type merge. In between, the system has undergone a metamorphosis. Scheffer calls this the plait-point transformation, and suggested that the point was situated on the unstable part of the critical line. Careful analysis by Baylé<sup>9</sup> shows that the point lies somewhat above the three-phase line. At this temperature and pressure, the tieline is connecting two points, both of which are on the spinodal. One point is the result of the two cusps meeting each other (called the beak to beak point in the language of catastrophe theory), and the other is the result of two spinodal–binodal crossing approaching each other. Despite their different “heritage”, the character of both points is of the same nature: both ends of the tieline lie on the spinodal.

The work of Scott and van Konynenburg is entirely based on the classical van der Waals equation for mixtures. For our considerations it is only necessary to assume that the Helmholtz free energy surface be expandable in a local Taylor series. The fact that points neighboring the critical line cannot be described that way has little influence, however, since the plait point is situated away from this region.

## 2. General Description: the Geometry of the A Surface

In order to establish the equilibrium between two phases in a thermodynamic system, a set of conditions, originally formulated by Gibbs, have to be fulfilled. These conditions can be described in geometrical terms, using the surface generated by the Helmholtz free energy. The Helmholtz free energy surface, at fixed temperature  $T$ , is given by a function  $A = A(T, V, x) = A_T(V, x)$ . In the three-dimensional isothermal  $A, V, x$  space this surface “descends from above”, because its slope is infinite on all four edges of the  $V(x)$  domain, one edge being  $V = \infty$  (ref 4).

At very high temperatures this surface is convex everywhere and undergoes deformations when the temperature is changed. Upon lowering of the temperature the surface may show a fold or plait, i.e., a concave region. The locus on the surface where the change in the sign of the curvature takes place is determined by the condition that the Hessian, the determinant of second derivatives of  $A(V, x)$ , is equal to zero (representing the parabolic points on the surface). The projection of this line on the  $V, x$  plane is the spinodal. Close to the regions of the  $A$  surface that are concave one may construct common tangent planes, i.e., planes that touch the surface at two (or more) different points in order to obtain the first-order phase transitions. The line that connects such points in space is called a tieline. The locus of the end points of these tielines is called the binodal or line of coexisting phases. Each pair of points satisfies the Gibbs conditions: equal pressure and equal chemical potentials. When the temperature is changed, which leads to a deformation of the surface, all these lines, the spinodals and the binodals, will change their positions.

To give a simple illustration of this behavior, consider a binary mixture of component 1 and component 2 at a temperature well below the critical temperature of component 1 as well as below the critical temperature of component 2. In this case there will be one simple (transverse) fold going from the left  $x = 0$  to the right  $x = 1$ . The concave region lies between the two branches of the spinodal: the vapor branch and the liquid branch. The binodal also consists of two branches, one above and one below the spinodal. The common tangent construction for values of  $0 < x < 1$  leads to a set of tielines that are no longer vertical for most of the intermediate values of  $x$ . Calculation of successive binodals can be done by a set of differential equations as given by Meijer.<sup>8</sup>

Upon further lowering of the temperature there might appear a vertical (longitudinal) plait. This fold is associated with liquid–liquid separation. Further deformation of the  $A$  surface will usually result in a three-phase equilibrium: that is, a tangent plane touches the surface in three points, creating a triangle consisting of three tielines as sides. Under these circumstances the binodals may cross the spinodals and consequently one observes single and double cusps which are the subject of the following considerations.

## 3. The Three Cases

Korteweg distinguished between three cases:<sup>10</sup> (1) both end points of the tieline are normal, i.e., nonparabolic, points; (2) one end point lies on a spinodal, i.e., is a parabolic point; (3) both ends of the tieline are situated on a spinodal. In the second case he showed that if one end lies on the spinodal, the other end shows a cusp. In the third case he demonstrates that the binodals are degenerate; i.e., there are two sets of binodals passing through each end and they are tangent to each other.

A description as to how case 2 goes over in case 3 is described in the literature. See for instance Scheffer.<sup>6</sup> Let us assume that the tieline goes from point 1 to point 2 on the free energy surface and that in the second case point 2 lies on the spinodal. As soon as point 1 approaches a spinodal, there appears an “image” of the cusp on the other side of the spinodal. When the surface is further distorted, these two cusps meet each other on the spinodal and annihilate each other (see Figure 4); near the meeting point the binodal becomes a double curve with a common tangent. At the same time, in the top part of the figures, the two binodals approach each other until they coincide. Upon still further distortion of the surface (compare Figure 4c), at

the neighborhood of the first point the tangent binodals show a separation while at the top the two cusps on each side of the spinodal are now pulling apart.

To sum it all up: it can be seen in a series of figures by van der Waals<sup>4</sup> that, upon slight changes in the parameters of the free energy function (such as occur when the temperature is changed), two opposing binodal cusps when meeting each other will form two curves that cross and osculate. This osculation takes place at the crossing with the spinodal. Subsequently, the binodal curves will separate from each other. At the same time the other end of the tieline the binodal curve will go through the opposite scenario. Two branches will coalesce and the cusps will retract from spinodal on each side of the spinodal. The net result is that the connectivity of the binodal system has been changed in such a way that the coalescence of two of the three phases will be differently arranged at the ends of the three-phase line. The local behavior is illustrated in Appendix A, using a simple analytical function.

The nonlocal behavior is more complicated than the simple example given for the local description. What happens at one end of the tieline is coupled to the behavior at the other end of the tieline. Note that the present calculation is beyond catastrophe theory, which deals with local situations only. In order to evaluate the behavior near the plait-point transformation, the three occurring configurations are considered first separately: (1) the binodal is separated from the spinodal at both ends of the tieline; (2) one end of the tieline moves through the spinodal while the other end does not; (3) both ends of the tielines cross segments of the spinodal simultaneously. Finally, the transition from case 2 into case 3 will be described.

#### 4. Calculation of the Three Cases

Let us assume that the Helmholtz free energy  $A$  can be expanded in a local Taylor series at each end of a given tieline as follows:

$$A_1 = a_0 + b_1x_1 + b_2y_1 + c_1x_1^2 + c_2x_1y_1 + c_3y_1^3 + d_1x_1^3 + d_2x_1^2y_1 + d_3x_1y_1^2 + d_4y_1^3 + e_1x_1^4 + \dots \quad (1)$$

$$A_2 = a'_0 + b'_1x_2 + b'_2y_2 + c'_1x_2^2 + c'_2x_2y_2 + c'_3y_2^2 + d'_1x_2^3 + d'_2x_2^2y_2 + d'_3x_2y_2^2 + d'_4y_2^3 + e'_1x_2^4 + \dots \quad (2)$$

where  $x_1, y_1$  are the coordinates around point 1 (the origin) and  $x_2, y_2$  the local coordinates around point 2. The local origin is at point 2 situated at  $x_1 = a, y_1 = 0$ , making the tieline into the  $x$ -axis. The length of the tieline is  $a$ . The common tangent plane is used as  $x$ - $y$  plane. Both series are slightly simplified by these choices. Since each of the origins are end points of the tieline, they must lie on the surface, hence  $a_0 = a'_0 = 0$ . The choice of the orientation of the common tangent plane results in  $b_1 = b_2 = b'_1 = b'_2 = 0$ . Finally, one may choose nonorthogonal (slanted) coordinates such that the coefficient  $c_2$  is made zero, as was done by Korteweg. Although this simplifies the calculation somewhat, it has the disadvantage that points 1 and 2 are no longer treated on an equal footing. We will use these coordinates only occasionally to simplify the description.

The physical meaning of the mathematical coordinates  $x$  and  $y$  depends on the orientation of the tieline. If one deals with a vapor-liquid type of separation,  $x$  represents the volume  $V$  and  $y$  the concentration  $x$ . In general  $x$  and  $y$  represent linear combinations of  $V$  and the concentration  $x$  as described in ref 11.

The three conditions of Gibbs for phase equilibrium as expressed in geometrical terms are as follows: The tangential and longitudinal derivatives as well as the chemical potentials should be equal at both ends. The last is obtained by means of the common tangent condition:

$$F \equiv \left(\frac{\partial A}{\partial x}\right)_1 - \left(\frac{\partial A}{\partial x}\right)_2 = 0 \quad (3)$$

$$G \equiv \left(\frac{\partial A}{\partial y}\right)_1 - \left(\frac{\partial A}{\partial y}\right)_2 = 0 \quad (4)$$

$$H \equiv A_1 - A_2 - (x_1 - x_2 - a) \left(\frac{\partial A}{\partial x}\right)_1 - (y_1 - y_2) \left(\frac{\partial A}{\partial y}\right)_1 = 0 \quad (5)$$

The Gibbs conditions (eqs 3, 4, and 5) are fulfilled at point 1 and point 2 (where  $x_1 = y_1 = 0$  and  $x_2 = y_2 = 0$ ). The conditions will now be used to calculate the binodals in the neighborhood of these two points.

**4.1. Case 1.** Consider first the solution for case 1 (no crossing of either branch of the binodal with the spinodal). This case is straightforward (see also ref 8) and is given only for comparison with cases 2 and 3.

Inserting the series 1 and 2 in the eqs 3, 4 and 5 gives, using the first order only

$$F = 0 \rightarrow 2c_1x_1 + c_2y_1 = 2c'_1x_2 + c'_2y_2 \quad (6)$$

$$G = 0 \rightarrow c_2x_1 + 2c_3y_1 = c'_2x_2 + 2c'_3y_2 \quad (7)$$

$$H = 0 \rightarrow 0 = 2c'_1x_2 + c'_2y_2 \quad (8)$$

These equations determine the linear part of the binodals:

$$y_1 = -(2c_1/c_2)x_1 \quad (9)$$

$$y_2 = -(2c'_1/c'_2)x_2 \quad (10)$$

as well as a relation between  $y_1$ , and  $y_2$  which governs the rate with which the ends of the tieline move along the binodal:

$$(1/2c_1)/\dot{y}_1 = (1/2c'_1)/\dot{y}_2 \quad (11)$$

introducing the Hessians in point 1 and point 2:

$$\dot{y}_1 \equiv 4c_1c_3 - c_2^2; \quad \dot{y}_2 \equiv 4c'_1c'_3 - c'^2_2 \quad (12)$$

Equations 9 and 10 illustrate the rule of the conjugated diameter as was derived by Korteweg. Higher order solutions can be obtained by introducing series expansions<sup>12</sup> in a parametric variable such as  $y_2$ :

$$x_1 = \sum_{n=1} Q_n y_2^n \quad (13)$$

$$y_1 = \sum_{n=1} R_n y_2^n \quad (14)$$

$$x_2 = \sum_{n=1} P_n y_2^n \quad (15)$$

This leads to the following expression for the first-order



coefficients:

$$P_1 = -c'_2/2c'_1 \quad (16p)$$

$$\frac{1}{c_2} \not\sim Q_1 = -\frac{1}{2c'_1} \not\sim; \quad \frac{1}{2c_1} \not\sim R_1 = \frac{1}{2c'_1} \not\sim \quad (16q,r)$$

Equations 16 give the local binodal in point 2. In order to obtain the local binodal in point 1,  $y_2$  has to be eliminated from eqs 16p and 16q, which leads again to eq 8. This may seem somewhat cumbersome, but the result can now be generalized in order to obtain higher order terms.

The second-order coefficients  $Q_2$ ,  $R_2$ , and  $P_2$  are determined by F2, G2, and H2:

$$2c_1Q_2 + c_2R_2 + 3d_1Q_1^2 + 2d_2Q_1R_1 + d_3R_1^2 = 2c'_1P_2 + 3d'_1P_1^2 + 2d'_2P_1 + d'_3 \quad (17 \text{ or F2})$$

$$c_2Q_2 + 2c_3R_2 + d_2Q_1^2 + 2d_3Q_1R_1 + 3d_4R_1^2 = c'_2P_2 + d'_2P_1^2 + 2d'_3P_1 + 3d'_4 \quad (18 \text{ or G2})$$

$$c_1Q_1^2 + c_2Q_1R_1 + c_3R_1^2 - (c'_1P_1^2 + c'_2P_1 + c'_3) = a[2c'_1P_2 + 3d'_1P_1^2 + 2d'_2P_1 + d'_3] \quad (19 \text{ or H2})$$

The last equation determines the value of  $P_2$ . The result can be expressed as follows:

$$2c'_1P_2 = -B'_x + \frac{L}{a} \quad (20)$$

introducing a shorthand for the following recurring expressions:

$$L \equiv c_1Q_1^2 + c_2Q_1R_1 + c_3R_1^2 - (c'_1P_1^2 + c'_2P_1 + c'_3) \quad (21)$$

the left-hand side of eq H2, and also

$$B'_x \equiv 3d'_1P_1^2 + 2d'_2P_1 + d'_3 \quad (22')$$

$$B'_y \equiv d'_2P_1^2 + 2d'_3P_1 + 3d'_4 \quad (23')$$

For later use  $B_x$  and  $B_y$  are introduced, the counterparts of the previous equations without the primes on the Taylor series coefficients (using  $s = -c_2/2c_1$ ):

$$B_x \equiv 3d_1s^2 + 2d_2s + d_3 \quad (22)$$

$$B_y \equiv d_2s^2 + 2d_3s + 3d_4 \quad (23)$$

Evaluation of  $L$ , using eqs 16 gives

$$L = \frac{\not\sim_2(c_1 \not\sim_2 - c'_1 \not\sim_1)}{4c'^2_1 \not\sim_1} \quad (24)$$

The right-hand side of eq 18 can be somewhat simplified using

$$R_{KW} \equiv B'_y + P_1B'_x = 3(d'_1P_1^3 + d'_2P_1^2 + d'_3P_1 + d'_4) \quad (25)$$

named after the factor  $R$  appearing in Korteweg's paper.<sup>10</sup> Hence

$Q_2$  and  $R_2$  are now determined by:

$$2c_1Q_2 + c_2R_2 = -B_xR_1^2 + \frac{1}{a}L \quad (26)$$

$$c_2Q_2 + 2c_3R_2 = -B_yR_1^2 + R_{KW} - P_1\frac{1}{a}L \quad (27)$$

which can be solved as long as  $\not\sim_1$  remains unequal to zero. If  $c_2$  is made zero, using the slanted coordinates introduced by Korteweg, then  $Q_1 = 0$  (see eq 16q) and eqs 26 and 27 need not be solved separately to obtain  $Q_2$  and  $R_2$ .

**4.2. Case 2.** The above results simplify as soon as  $\not\sim_2 = 0$ , leaving  $\not\sim_1 \neq 0$  for the moment. Since

$$L = 0; \quad R_1 = 0; \quad Q_1 = 0 \quad (28)$$

one obtains

$$\not\sim_1Q_2 = -c_2R_{KW}; \quad \not\sim_1R_2 = 2c_1R_{KW} \quad (29a,b)$$

To find the behavior of the binodal near point 1, one must eliminate  $y_2$  from

$$x_1 = Q_2y_2^2 + Q_3y_2^3 + \dots; \quad y_1 = R_2y_2^2 \dots \quad (30)$$

leading to

$$2c_1x_1 + c_2y_1 = 2c_1Q_3(y_1/R_2)^{3/2} \quad (31)$$

this represents a cusp as was observed by Korteweg (ref 10).

If one uses slanted coordinates such that  $c_2 = 0$ , the coefficient  $Q_2$  will be zero according to eq 26 and  $R_2 = R_{KW}/2c_3$ . The cusp now has a tangent along the  $y$ -axis, and furthermore

$$s = 0; \quad B_x = d_3; \quad B_y = 3d_4 \quad (33)$$

The case  $\not\sim_2 \neq 0$ , and  $\not\sim_1 = 0$  will require a new choice of the parameter in eqs 13–15.

**4.3. Case 3.** The solution changes drastically when  $\not\sim_1 = 0$  also, and many of the equations have to be revised. In the first-order calculation  $P_1$  remains the same, but  $Q_1$  and  $R_1$  are no longer determined, except for a linear relation between them:  $Q_1 = sR_1$ . The coefficient  $R_1$  is determined by the second-order calculation and it is double valued.

The second-order calculation for  $P_2$  is the same because the left-hand side of eq 19 is again zero. The result for the other coefficients is determined by

$$2c_1Q_2 + c_2R_2 = -B_xR_1^2 \quad (34)$$

$$c_2Q_2 + 2c_3R_2 = -B_yR_1^2 + R_{KW} \quad (35)$$

which is the same as eq 26 and eq 27 with  $L = 0$ . However, these equations contradict each other, unless

$$\frac{2c_3}{c_2}B_xR_1^2 = B_yR_1^2 - R_{KW} \quad (36)$$

which leads to

$$R_1^2 = \frac{R_{KW}}{sB_x + B_y} = \frac{d'_1P_1^3 + d'_2P_1^2 + d'_3P_1 + d'_4}{d_1s^3 + d_2s^2 + d_3s + d_4} \quad (37)$$

and the relation between  $Q_2$  and  $R_2$  is given by eq 34. One can

determine  $Q_2$  and  $R_2$  separately only in a third-order calculation. The coefficients  $R$  and  $Q$  lag one order behind in each step in the calculation of case 3.

Taking  $c_2 = 0$  one obtains, after elimination of  $y_2$ :

$$x_1 = -\frac{B_x}{2c_1}y_1^2 \quad (38)$$

which is a parabola. Calculation of the next order coefficient in  $y_1$  shows that this coefficient has two values. The two parabolas osculate; i.e., they have a common tangent.

**4.4. Intermediate Case, between 2 and 3.** Condition  $H$ , the common tangent condition, determines the coefficients  $P_1$ ,  $P_2$ , and  $P_3$  independently of the coefficients  $Q$  and  $R$ . The first two are given in eq 16p and in eq 20 (with  $L = 0$ ). Using these results one may evaluate the right-hand sides of conditions F and G and one obtains, ignoring the strict hierarchy with which first- and second-order terms were treated previously:

$$2c_1x_1 + c_2y_1 + B_x y_1^2 = Q_3 y_2^3 \quad (39)$$

$$c_2x_1 + 2c_3y_1 + B_x y_1^2 = R_{KW} y_2^2 \quad (40)$$

since elimination of  $x_1$  leads to

$$\mathcal{H}_1 y_1 + (2c_1 B_y - c_2 B_x) y_1^2 = 2c_1 R_{KW} y_2^2 + (\text{third order in } y_2) \quad (41)$$

This equation can be written as

$$y_2^2 = \frac{\mathcal{H}_1}{2c_1 R_{KW}} y_1 + \frac{1}{R_1} y_1^2 \quad (42)$$

If this is substituted in eq 39, one obtains

$$2c_1x_1 + c_2y_1 + B_x y_1^2 = Q_3 \left( \frac{1}{R_2} y_1 + \frac{1}{R_1} y_1^2 \right)^{3/2} \quad (43)$$

if eq 29b is used. For  $\mathcal{H}_1 \gg 0$  one regains eq 31 since  $y_1^{3/2}$  dominates over the  $y_1^2$  term, while for  $\mathcal{H}_1 = 0$  the  $B_x$  term takes over and one recovers eq 38 when  $c_2 = 0$ . Analysis of this equation shows that there is a second cusp at

$$y_1^c = -\frac{R_1^2}{R_2} = \frac{\mathcal{H}_1}{2c_1 B_y - c_2 B_x} \quad (44)$$

besides the one at  $y_1 = 0$ . For  $c_2 = 0$  this simplifies to  $y_1^c = -2c_3/d_4$ . This second cusp will merge with the cusp at the origin when  $c_3$ , or in general  $\mathcal{H}_1$ , goes to zero.

## 5. Distortion of the A Surface

In the preceding sections, the quantity  $c_3$  or  $\mathcal{H}_1$  was taken as a variable parameter. There are, however, many different ways the surface may deform. An alternate way to consider the problem is to assume that initially one deals with case 3: the tieline connects two (double) binodals which both cross the spinodal at the ends of the tieline. Assume now that the surface is deformed such that the coefficients  $b_1$ ,  $b_2$  and  $b'_1$ ,  $b'_2$  are no longer zero, but keeping  $\mathcal{H}_1 = 0$ . The plane is no longer a common tangent plane and the Gibbs conditions are not fulfilled, and consequently the connector between the points 1 and 2 is no longer a tieline. By moving both ends of this connector over a small distance over the deformed surface, such that the Gibbs

conditions are satisfied again at the end points, the connector can be made again into a tieline.

Assuming, as before, that both ends of the connector are still on the A surface, one has again  $a_0 = 0$  and  $a'_0 = 0$ . Assuming furthermore that both ends of the connector are located on spinodals, one now moves the point 2 to 2' (vector components  $u'$  and  $v'$ ) along the spinodal and displaces the point 1 to 1' (vector components  $u$  and  $v$ ), such that the Gibbs conditions are restored. Keeping the point 2 on the spinodal requires

$$c'_1 B'_x u' = -c'_3 B'_y v' \quad (45)$$

and eq 5, the third Gibbs condition, requires

$$ab'_1 + a(2c_1u + c_2v) + (b_1 - b'_1)u' + (b_2 - b'_2)v' = 0 \quad (46)$$

Hence the first-order results for  $u'$  and  $v'$  are

$$u' = \frac{c'_3 B'_y}{c'_3 B'_y (b_1 - b'_1) - c'_1 B'_x (b_2 - b'_2)} a(b'_1 + 2c_1u + c_2v) \quad (47a)$$

$$v' = -\frac{c'_1 B'_x}{c'_3 B'_y (b_1 - b'_1) - c'_1 B'_x (b_2 - b'_2)} a(b'_1 + 2c_1u + c_2v) \quad (47b)$$

The first two Gibbs conditions lead to

$$b_1 + 2c_1u + c_2v + 3d_1u^2 + 2d_2uv + d_3v^2 = b'_1 + 2c'_1u' + c'_2v' + 3d'_1u'^2 + 2d'_2u'v' + d'_3v'^2 \quad (48F)$$

$$b_2 + c_2u + 2c_3v + d_2u^2 + 2d_3uv + 3d_4v^2 = b'_2 + c'_2u' + 2c'_2v' + d'_2u'^2 + 2d'_3u'v' + 3d'_4v'^2 \quad (48G)$$

Since the linear parts of these equations are dependent, the Korteweg method for the solution of second-order equations will be used again; i.e., one makes the assumption

$$u = sv + \mathcal{P} \quad (49)$$

where  $\mathcal{P}$  has to be determined. This leads to two equations

$$2c_1 \mathcal{P}^2 + B_x v^2 = R_F \quad (50F)$$

$$c_2 \mathcal{P}^2 + B_y v^2 = R_G \quad (50G)$$

where  $R_F$  is the right-hand side of eq 48F and similar for G. Elimination of  $\mathcal{P}$  leads to

$$v = \pm \left[ \frac{sR_F + R_G}{sB_x + B_y} \right]^{1/2}; u = sv \quad (51)$$

that means there are two solutions for the point 1', the tips of the cusp. They are situated on opposing sides of the spinodal at equal distance and they lie on the cylindrical axis of the parabolic point of the spinodal. The corresponding points at the other end of the tielines are still coinciding in the first-order calculation.

In order to give an idea as to what determines the type of break-up that will occur near the beak-to-beak point upon distortion of the surface (i.e., two cusps versus two parallel binodals), we assume that  $c_2 = 0$ . Using the eqs 33, one obtains

$$v = \pm [R_G/3d_4]^{1/2} \quad (51a)$$

The factor  $R_G$  is approximately given by

$$R_G \approx b'_2 + \mathcal{Q}b'^2_2 \quad (52)$$

hence the sign of  $b'_2$  (actually the sign of  $b'_2 - b_2$ ) will determine whether  $v$  is real or imaginary, since the coefficient  $d_4$  is not likely to change very much upon distortion of the surface. If  $v$  is real, the beak-to-beak will separate in two cusps at the point 2, each with their own spinodal–binodal crossing near point 1. If, by contrast, the argument of the square root is negative, the calculation has to be redone with the role of point 1 and point 2 interchanged, leading to the separation into two cusps at point 1.

## 6. Observation

Can the point  $M$  ever be observed? Definitely not by scanning through equilibrium states, but probably by detecting the metastable end points. The metastable region in the  $V(x)$  or  $p(x)$  diagram is the region between the outermost contour of the binodal lines and the spinodal. Not all segments in this region are metastable. Only the segments that start at the binodal self crossing points up to the spinodal or to a cusp. (Segments between a cusp and the spinodal may belong to the metastable region, but their counterparts, at the other end of the tieline do not, and hence these points are unstable.) If the metastable end point lies on the spinodal, then the density will have a maximum (or a minimum).

For  $T_{\text{LCEP}} < T < T_M$  the metastable branch  $C'B''$  (compare Figure 2) ends in a maximum on the right-hand side of the tieline, but not on the left side of the tieline because there the metastable branch ends in a cusp, and hence the fluctuations will be more concentration-like. This is because the end point of the metastable state at a maximum value of  $p(x)$  lies in this case on the high  $x$  and low  $V$  (or liquid) side. For  $T_M > T > T_{\text{UCEP}}$  we have the reverse. The fluctuations will be more density-like. It must be possible to observe the differences experimentally as follows:

If the system is in a metastable two-phase state at a temperature in the range  $T_{\text{LCEP}} < T < T_M$ , the fluctuations will take place below the existing meniscus and the new meniscus will eventually appear in the lower part of the system under observation. For a temperature above  $T_M$  the opposite will happen. At  $T = T_M$  fluctuations will take place above and below the meniscus and it is conjectured that the meniscus will probably “split” in two parts.

At the point  $M$  the fluctuations are probably exceptionally large. This may be of use in systems that have trouble separating out. The point  $M$  can be determined provided the equation of state is known. This in turn determines the binodals as a function of the temperature. A metastable state could be obtained by rapid change in  $T$ , but also by rapid change in  $p$  (at constant  $T$ ).

## 7. Conclusion

In this section a very general description of the plait-point transformation is given by following the behavior of the closed loop binodal in relation to the main binodal in the  $V(x)$  plots. In what follows the expressions horizontal and vertical have to be read as “more or less horizontal” and “more or less vertical”. Hence a horizontal tieline actually refers to a tieline between two points with very different values of  $x$ , but with rather small differences in the values of  $V$ . At low temperatures there may develop a closed loop with horizontal tielines situated inside the main bulge. The tielines of this closed loop and the critical

points that go with it all lie in the unstable region. Upon increasing the temperature, this loop may move vertically and as soon as it pops out of the main loop one deals with a horizontal stable tieline, which is the top part of the triangle that forms the three-phase state. This describes the situation before the plait-point transformation takes place and is given in Figure 2. When the transformation takes place all binodals are completely connected and there is no distinction between the main bulge and an additional closed loop. After the transformation, the new closed loop that emerges has vertical tielines and the two crossing points of the new closed loop and the main bulge are now the vertical side of the three-phase triangle. When this loop starts to retract into the main bulge, this side of the tielines contracts and this implies the merging of a the liquid and vapor phase at the UCEP.

**Acknowledgment.** I thank Dr. Th. W. de Loos for bringing the thesis of Baylé to my attention and I thank the Physical and Chemical Properties Division of the National Institute of Standards and Technology for their hospitality as a guest worker.

## Appendix A

**Example of a Function That Shows the Changeover from “Beak to Beak” to Osculation to Separation.** Osculating curves are curves that have a point in common and have the same tangent at that point. The analytical expression used to illustrate this behavior is

$$y^2 = (x^2 + b)^3 \quad (A.1)$$

where  $b$  is a parameter which will be varied. For negative  $b = -a^2$  one obtains one obtains two opposing cusps at the points  $x = a$  and  $x = -a$  (see ref 3, Figure 5a). For large  $a$  one obtains

$$y \approx \pm(2a(x \mp a))^{3/2} \quad (A.2)$$

When  $b$  goes to zero the two cusps will meet. In this case the two curves have a common tangent in the origin. For positive  $b$ , the curves will separate and the distance in height between the curves is equal to  $2b^{3/2}$  (see ref. 3, Figure 5b). The vertical axis represents the spinodal because the Hessian equals zero on this locus. This illustration is incomplete since it deals with one end of the tieline only.

## Appendix B

**Taylor Series with Vanishing Leading Coefficient.** The intermediate case is governed by the changeover in behavior of a Taylor series with vanishing leading coefficient. Consider the series

$$y = ax + bx^2 + cx^3 + \dots \quad (B.1)$$

with  $a \rightarrow 0$ . The solution  $x = x(y)$ , i.e., inversion of this series is straight-forward (see NBS Handbook) as long as  $a \gg 0$  (or  $a \ll 0$ ), but is of entirely different nature when  $a = 0$ , leading to a Puiseux series.

In order to obtain a solution of the problem for small but nonzero  $a$ , one may use a displacement of the origin. Ignoring for the moment the coefficient  $c$  eq B.1 gives

$$y' = y + \frac{a^2}{4b} = bx'^2 \quad \text{with } x' = x + \frac{a}{2b} \quad (B.2)$$

The inversion is now similar, to the  $a = 0$  case. The same method can be used when the third-order and higher terms are

introduced. The first step is to shift the  $x$ -coordinate:  $x' = x - \delta$ . The next step is to suppress the first-order coefficient. This leads to

$$a + 2bd\delta + 3c\delta^2 + \dots = 0 \quad (\text{B.3})$$

which is solved by a series inversion leading to  $\delta(a)$ . This is substituted in the original series. The constant term is now

$$a\delta + b\delta^2 + c\delta^3 + \dots \quad (\text{B.4})$$

and similar renormalization for the coefficients  $b, c, \dots$ . The need for this expansion comes from the proximity of second root for  $y = 0$ ; besides  $x = 0$  one obtains  $x = -b/a$  which for large  $a$  can be ignored, making the procedure unnecessary, if not unwanted.

## References and Notes

- (1) van Konynenburg, P. H.; Scott, R. L. *Philos. Trans. R. Soc.* **1980**, 298, 495–594.
- (2) Scheffer, F. E. C. *Heterogene Evenwichten in Unaire en Binaire Stelsels (Heterogeneous Equilibria in Simple and Binary Systems)*, 2nd ed.; Waltman: Delft, The Netherlands, 1960.
- (3) Meijer, P. H. E. The metamorphosis from LCEP to UCEP in the metastable three-phase region in type-V phase diagrams. *Conf. Proc. 8th Int. Conf. Properties Phase Equilib. Product Process Des.*, *Fluid Phase Equilib.* **1999**, Vols. 158–160.
- (4) van der Waals, J. D.; Kohnstamm, Ph. A. *Lehrbuch der Thermodynamik, Vol. II, Binäre Gemische*; Barth: Leipzig, Germany, 1912; second ed. 1927.
- (5) van der Waals, J. D. *Arch. Néerlandaises Sci. Exactes Naturelles* **1891**, 24, 1–56. See also Rowlinson's translation.
- (6) Scheffer, F. E. C. *Proc. Sci. Sec., Kon. Ned. Akad.* **1912–1913**, 15 (1st part), 389–405.
- (7) Korteweg, D. J. *Arch. Néerlandaises Sci. Exactes Naturelles* **1891**, 24, 295–368.
- (8) Meijer, P. H. E. *Physica A* **1997**, 237, 31–44. Note: In this paper the expressions “longitudinal” and “transverse” were accidentally interchanged on p 39.
- (9) Baylé, G. G. *Evenwichten bij Hoge Druk tussen Fluide Phasen in Binaire en Ternaire Systemen met Ontmenging (Equilibria at high pressures in binary and ternary systems with demixing)*; Excelsiors Foto-Offset: Gravenhage, 1951.
- (10) Korteweg, D.J. *Mathematical Problems with Solutions of the Society (with the motto) E.O.A.K.A.T.B.* **1890**; Tome IV, problems nos. 87–89, pp 331–338. (The initials stand for: Untiring labor shall overcome everything.)
- (11) Meijer, P. H. E. *J. Chem. Phys.* **1994**, 101, 5140–5147.
- (12) The author would like to express his thanks to Dr. A. H. M. Levelt of the Katholieke Universiteit in Nijmegen, who taught me how to set up this type of solution in a systematic way.